Analytical and numerical study of validation test-cases for multi-physic problems: application to magneto-hydro-dynamic*

David Cébron[1] and Jean-François Sigrist[2]
[1]Ecole Centrale de Nantes, Rue de la Noë, 44 621 Nantes, France
[2]DCNS Propulsion, Service Technique et Scientifique, 44620 LA Montagne, France
E-mail: jean-francois.sigrist@dcnsgroup.com

ABSTRACT

The present paper is concerned with the numerical simulation of Magneto-Hydro-Dynamic (MHD) problems with industrial tools. MHD has received attention some twenty to thirty years ago as a possible alternative in propulsion applications; MHD propelled ships have even been designed for that purpose. However, such propulsion systems have been proved of low efficiency and fundamental researches in the area have progressively received much less attention over the past decades. Numerical simulation of MHD problem could however provide interesting solutions in the field of turbulent flow control. The development of recent efficient numerical techniques for multi-physic applications provide promising tool for the engineer for that purpose. In the present paper, some elementary test cases in laminar flow with magnetic forcing terms are analysed; equations of the coupled problem are exposed, analytical solutions are derived in each case and are compared to numerical solutions obtained with a numerical tool for multi-physic applications. The present work can be seen as a validation of numerical tools (based on the finite element method) for academic as well as industrial application purposes.

Keywords: Finite element method, multi-physic simulation; magneto-hydro-dynamic.

1. INTRODUCTION

Magneto-Hydro-Dynamic (MHD) effects have received attention some twenty to thirty years ago as a possible alternative in propulsion applications; MHD propelled ships have even been designed for that purpose: the most famous example is the Japanese ship Yamamoto 1, which has been designed and build as prototype of MHD-propelled ship (see Fig. 1 featuring a photo of the MHD thrusters of Yamamoto 1). However such propulsion systems have been proved of low efficiency and fundamental researches in the area have progressively received much less attention over the past decades.

*The present paper is based on a previous contribution in the "Multiphysic" session at the "Emerging Technology in Fluid, Structure and Fluid-Structure Interaction" symposium at the "Pressure Vessel and Piping" conference, held in Chicago on July 2008 (D. Cébron, J.F. Sigrist, V. Soyer, P. Ferrant. *Validation Test-Cases for Multi-Physic Problems: Application to Magneto-Hydro-Dynamic Numerical Simulations*. Pressure Vessel and Piping, Chicago, 27–31 July 2008.).

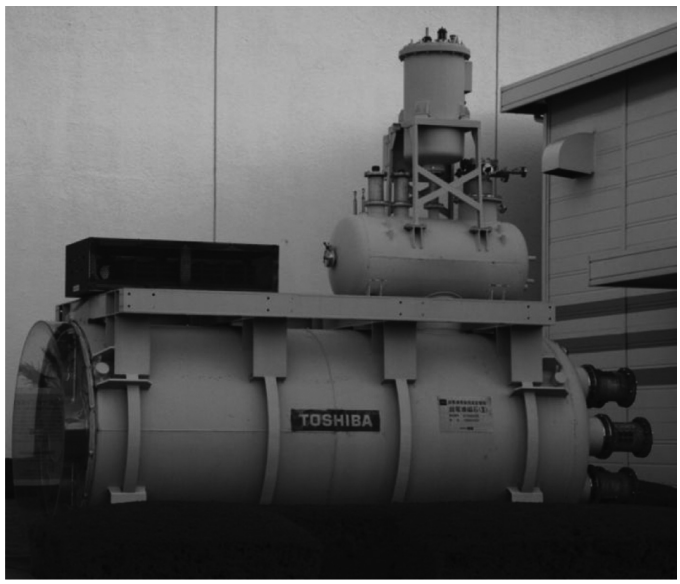

Figure 1 A MHD thruster from the experimental Japanese ship Yamato 1 at the Ship Science Museum in Tokyo.

Numerical simulation of MHD problem could however provide interesting solutions in the field of turbulent flow control. The development of recent efficient numerical techniques for multi-physic applications provide promising tool to the engineer for that purpose. In the present paper, elementary test cases involving various MHD effects are studied: the general equations of MHD coupled problems are first recalled (section 2); then, analytical test-cases in laminar flow with magnetic forcing terms are analysed, namely the "Hartman problem" (section 3), the "Couette problem" (section 4) and the "Rayleigh problem" (section 5). An analytical solution is derived in each case and serves as a reference for comparison with a numerical solution obtained from a numerical tool for multi-physic applications.

2. MDH PROBLEM: GENERAL FORMULATION AND NUMERICAL RESOLUTION

2.1. OVERVIEW OF THE MHD EQUATIONS

A general description of a MHD problem is derived from the following set of fundamental equations [1,2]. Let v be the velocity of the fluid flow, whose physical characteristics are denoted ρ (density), η (viscosity), and σ and λ (electrical and thermal conductivity). Let **j** be the current density field and **E** and **B** the electric and magnetic fields; let ε be the electric charge density, e the energy per unit mass of the fluid and r the volumic source of heat. $\mathbf{D}_r$ and $\mathbf{B}_r$ respectively stand for the remanent displacement and the remanent magnetic flux density. The ground equations for a general MHD problem are written as follows:

- Ohm equation:

$$\mathbf{j} = \sigma(\mathbf{E} + \mathbf{v} \times \mathbf{B}) \tag{1}$$

- Navier Stokes equation:

$$\frac{\partial \rho}{\partial t} + \nabla \cdot (\rho \mathbf{v}) = \frac{D\rho}{Dt} + \rho \nabla \cdot \mathbf{v} = 0 \tag{2}$$

- Maxwell equations:

$$\nabla \times \mathbf{E} = -\frac{\partial \mathbf{B}}{\partial t} \tag{3}$$

$$\nabla \times \left(\frac{\mathbf{B} - \mathbf{B}_\mathbf{r}}{\mu} \right) = \mathbf{j} + \frac{\partial \left(\varepsilon \mathbf{E} + \mathbf{D}_\mathbf{r} \right)}{\partial t} \tag{4}$$

$$\nabla \cdot \mathbf{B} = 0 \tag{5}$$

$$\nabla \cdot \mathbf{E} = \varepsilon \tag{6}$$

The equation of momentum for the fluid reads:

$$\rho \frac{D\mathbf{v}}{Dt} = \mathbf{j} \times \mathbf{B} - \nabla p + \eta \Delta \mathbf{v} \tag{7}$$

when the advective terms have been discarded, and the equation of energy for the fluid is written as:

$$\frac{\rho}{\lambda} \frac{De}{Dt} = \Delta T + \frac{\eta}{\lambda} \left\| \nabla \mathbf{v} + \nabla \mathbf{v}^T \right\|^2 + \frac{\mathbf{j} \cdot \mathbf{E}}{\lambda} + \frac{r}{\lambda} \tag{8}$$

with viscous and ohmic dissipation, assuming that density, viscosity, electrical and thermal conductivity of the fluid are not temperature-dependant.

2.2. NUMERICAL TECHNIQUE FOR MULTI-PHYSIC PROBLEMS

It is obviously not possible to derive an analytical solution of the above formulated system of equations, except in some particular configurations, some of which are studied in the present paper.

Numerical simulation is therefore of practical use in such complex multi-physic configuration; among a large variety of numerical tools available to the engineer for industrial applications, COMSOL-Multiphysics is one of the most popular and powerful tool which can be employed to tackle multi-physic problems, see Fig. 2. It is a finite element method-based code, which allows for multi-physic simulations, using a set a elementary solvers, which can be coupled in various ways. Solving the above equations with a finite element method requires the discretisation of a weak formulation of the problem. In the present context of MHD equations, the basic discretisation principles are as follows. Given that the fluid is incompressible, Eq. (2) can be written as:

$$\int_S \left[\frac{\partial \rho}{\partial t} + u \frac{\partial \rho}{\partial x} + v \frac{\partial \rho}{\partial y} \right] \tilde{\rho} \cdot ds = 0 \tag{9}$$

while the equation of the motion can be reformulated as:

$$\rho \frac{D\mathbf{v}}{Dt} = \nabla \cdot \left[-p\bar{\bar{I}} + \eta \bar{\bar{d}} \right] + \mathbf{j} \times \mathbf{B} \tag{10}$$

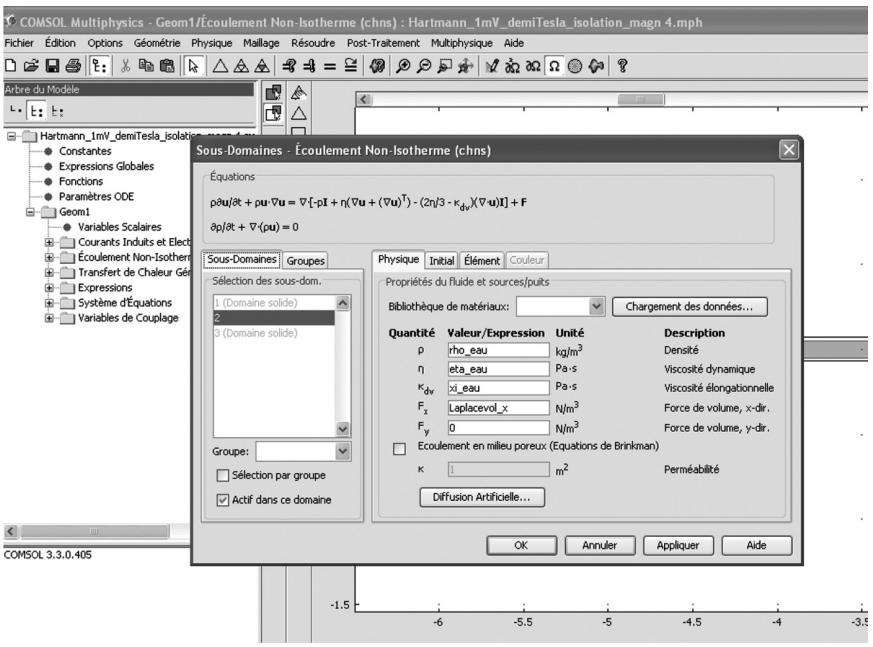

Figure 2 Implementation of the MHD equations in the COMSOL-Multiphysic numerical tool.

Taking the state equation of an incompressible fluid $e = C_v T$ (with C_v being the specific heat at constant volume), which is also the state equation of an ideal gas Eq. (8) can be written as:

$$\int_S \left[\rho \cdot C_p \cdot \tilde{T} \right] dx = \int_S \left[\lambda \cdot \left(\frac{\partial T}{\partial x}\frac{\partial \tilde{T}}{\partial x} + \frac{\partial T}{\partial y}\frac{\partial \tilde{T}}{\partial y} \right) + q_v \tilde{T} - \rho \cdot C_v \cdot \tilde{T} \left(u\frac{\partial T}{\partial x} + v\frac{\partial T}{\partial y} \right) \right] dx \tag{11}$$

In order to solve the partial differential system of Maxwell equations, these equations are gathered into two equations. One can notice that if there is an extern magnetic field B_o, which is the case in this study, this field is considered as a remanent magnetic flux density.

From the Faraday law, it is possible to derive an electric scalar potential V defined by [1,2,3]:

$$\mathbf{E} = -\nabla V - \frac{\partial \mathbf{A}}{\partial t} \tag{12}$$

From the Gauss law, it is possible to derive a magnetic vector potential $\mathbf{A}$ defined by [1,2,3]:

$$\mathbf{B} = \nabla \times \mathbf{A} \tag{13}$$

Subsequently, it is possible to formulate the problem only in terms of potentials V and $\mathbf{A}$. Equations (4) and (1) can be indeed written as:

$$\left(\sigma+\varepsilon\frac{\partial.}{\partial t}\right)\frac{\partial \mathbf{A}}{\partial t}+\nabla\times\left(\frac{\nabla\times\mathbf{A}-\mathbf{B_r}}{\mu}\right)-\sigma\mathbf{v}\nabla\times\left(\nabla\times\mathbf{A}\right)+\left(\sigma+\varepsilon\frac{\partial.}{\partial t}\right)\nabla V=\frac{\partial \mathbf{D_r}}{\partial t} \tag{14}$$

Taking into account the divergence of Eq. (4), and substituting in Eq. (1) yields:

$$\nabla\cdot\left[\left(\sigma+\varepsilon\frac{\partial.}{\partial t}\right)-\sigma\mathbf{v}\nabla\times\left(\nabla\times\mathbf{A}\right)+\left(\sigma+\varepsilon\frac{\partial.}{\partial t}\right)\nabla V-\frac{\partial \mathbf{D_r}}{\partial t}\right]=0 \tag{15}$$

In the present study, the electromagnetic problem is solved using the two preceding equations for a stationary two-dimensional problem in assuming that $\mathbf{D}_r = 0$. With the previous weak formulation of equations, in meshing the space, the problem can be solved in solving the non-linear system of equations, from the discretization on the nodes, to minimize residuals of a finite elements method. The whole process is carried out with the COMSOL-Multiphysic numerical tool, using the appropriate modules.

Validation of the multi-physic numerical method being the key-issue of the procedure, the present paper focuses on comparison between numerical calculations and analytical solutions which are derived for elementary test cases. From the technical point of view, further information on the COMSOL-Multiphysic numerical tool can be found in a first approach by browsing on the website www.comsol.fr and related publications; from the scientific point of view, some ground consideration on coupling techniques for MHD simulations can be found in reference [4].

3. HARTMANN PROBLEM

The first elementary test case considered in the present investigation is the so-called "Hartmann problem", represented in see Fig. 3 bellow. It is reminded that the problem to be considered is the steady flow of an incompressible electrically conducting fluid in the positive x direction, with an extern magnetic field $\mathbf{B}_o$, assumed to be uniform and constant, in the positive z direction. Assuming an electrical conductivity infinite for the electrodes, end effects ($L>>a$), secondary flows ($b>>a$) and the Hall effect can safely be neglected.

Except for the pressure p and the temperature T, previous assumptions lead to variables functions of alone, which are thus expresses as $\mathbf{v} = (u_x, 0, 0)$, $\mathbf{j} = (0, j_y, 0)$, $\mathbf{B} = (b_x, 0, B_o)$, $\mathbf{E} = (0, E_o, 0)$, where E_o and B_o are constants.

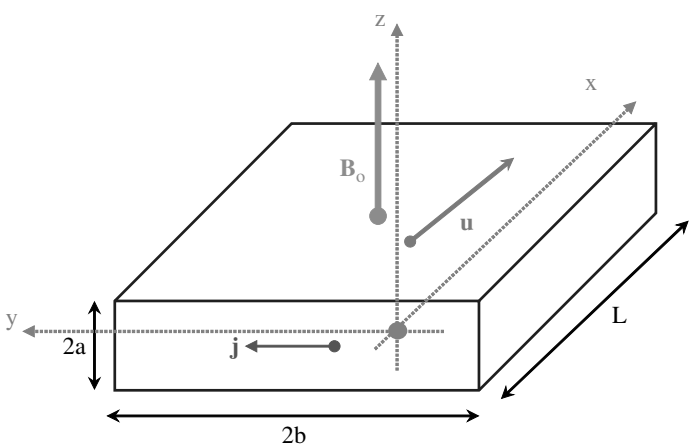

Figure 3 Definition of the MHD "Hartmann problem".

These legitimate hypotheses allow obtaining analytical solution and simplifying the numerical simulation. In the first three cases studied in this paper, the flow can be solved in two dimensions. However, at first sight, this problem has to be similar to the theoretical one, and therefore, a normal current, whose profile is unknown, has to be set: the profile is solved in the direction of the magnetic field.

After analysis of the equations above, in the first three particular cases studied, the equations are found to be invariant by permutation of the electrical end magnetic field. Then, a normal uniform magnetic field is used in the numerical simulation, and the flow is solved in the direction of the unknown current. It should nonetheless be noticed that this assumption is not true in general, for instance in problems involving a finite-length duct.

3.1. ANALYTICAL SOLUTION FOR THE HARTMANN PROBLEM

Since the heat-transfer and fluid motion equations are uncoupled for an incompressible fluid, it is possible to solve the corresponding equations in a separate manner. Moreover, since the equations are linear the solution for the velocity profile u_x and the mean velocity $\overline{u}$ is found to be [1]:

$$U = \frac{u_x}{\overline{u}} = \mathrm{H}\,\frac{\mathrm{ch}(\mathrm{H}) - \mathrm{ch}(\mathrm{ZH})}{\mathrm{Hch}(\mathrm{H}) - \mathrm{sh}(\mathrm{H})} \tag{16}$$

$$\overline{u} = \frac{\mathrm{H} - th(\mathrm{H})}{\mathrm{H}^3} \times \left(\mathrm{H}^2 \frac{E_o}{B_o} - \frac{a^2}{\eta} \frac{\partial p}{\partial x} \right) \tag{17}$$

with boundary condition $u_x(\pm a) = 0$. In the preceding expression, the non-dimensional ratios Z and H are defined as $\mathrm{Z} = \frac{z}{a}$ and $\mathrm{H} = aB_\mathrm{o}\sqrt{\frac{\sigma}{\eta}}$; the latter is the so-called Hartmann number. ch(•) and *s*h(•) stand for hyperbolic cosine and sine, respectively. Figure 3 plots some typical velocity profile within the duct in the Hartmann problem, for various H; it is stressed that the case H = 0 corresponds to the situation where magnetic forcing is absent.

It is interesting to bear in mind that a number of experimental investigations have provided excellent agreement with the previous solution (see for instance [2]). Letting $K = \frac{E_o}{\overline{u}B_o}$ be the load factor of the flow and J the net current flowing through the circuit per unit area, it is possible to deduce the reduced $\tilde{j}_y$ and the net density J of currents:

$$\tilde{j}_y = \frac{j_y}{\sigma \overline{u} B_o} = K - \frac{u_x}{\overline{u}}, \quad J = (K-1)\sigma \overline{u} B_o \tag{18}$$

The electric field E_o generated by a tension Ω, is obtained here with Eq. (6) in the case of a parallel-wall channel $E_o = \frac{\Omega}{2b}$. The reduced induced magnetic field $\tilde{b}_x$ is derived from Eq. (4):

$$\tilde{b}_x = \frac{b_x}{B_o \mathrm{R_m}} = (K-1)Z + \frac{\mathrm{sh}(\mathrm{HZ}) - Z\,\mathrm{sh}(Z)}{\mathrm{H\,ch}(\mathrm{H}) - \mathrm{sh}(\mathrm{H})} \tag{19}$$

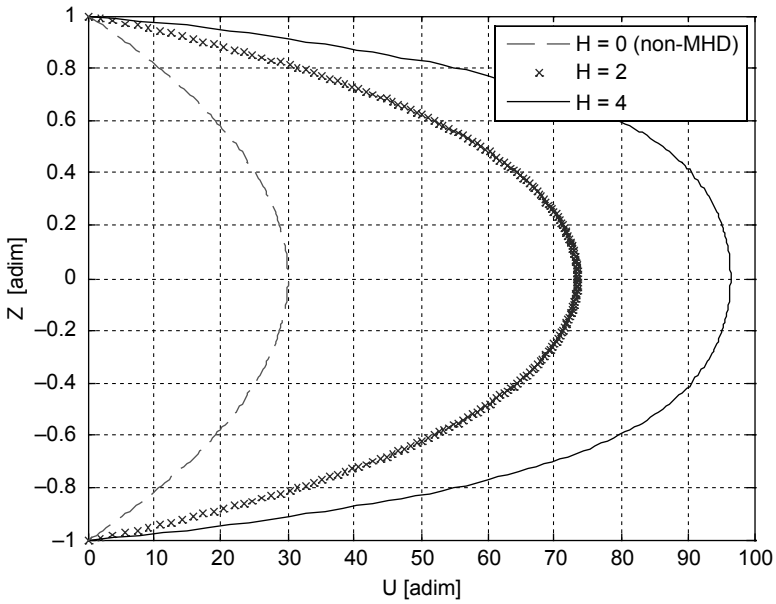

Figure 4 Analytical velocity distribution for the Hartman problem (with Kxu=100).

where, as a consequence of symmetry of the problem, the boundary condition for b_x is assumed to be $b_x = 0$.

The magnetic Reynolds number R_m is defined here as $\mathrm{R_m} = \dfrac{a\bar{u}}{D_{\mathrm{mag}}}$, where $D_{\mathrm{mag}} = \dfrac{1}{\mu\sigma}$ is the magnetic diffusivity. Taking the state equation of an incompressible fluid $e = C_v T$ (with C_v being the specific heat at constant volume), which is also the state equation of an ideal gas (second Joule's law), Eq. (8) can be written as $\lambda \dfrac{\partial^2 T}{\partial z^2} + \eta \left(\dfrac{\partial u_x}{\partial z} \right)^2 + \dfrac{j_y^2}{\sigma} + r = 0$, hence the equation for temperature:

$$\frac{\partial^2 \theta}{\partial Z^2} = -\mathrm{P_r} \left[\left(\frac{\mathrm{dU}}{\mathrm{dZ}} \right)^2 + \mathrm{H}^2 \tilde{j}_y^2 \right] - \tilde{r} \tag{20}$$

with the reduced temperature $\theta = \dfrac{C_v}{\bar{u}^2}(T - T_w)$ (which can be seen as the ratio between the thermal energy of the fluid and its kinetic energy), Prandtl number of the fluid $\mathrm{P_r} = \dfrac{\eta C_v}{\lambda}$, and the reduced source of heat $\tilde{r} = r \dfrac{C_v a^2}{\lambda \bar{u}^2}$.

The boundary condition for T is assuming to be $T(\pm a) = T_w$, so that the analytical solution of Eq. (20) is:

$$\theta = C_1 \mathrm{P_r} \left[\frac{C_2^2}{2}(1 - Z^2) + \frac{1}{4}\left(\mathrm{ch}(2\mathrm{H}) - \mathrm{ch}(2\mathrm{H}Z)\right) + \frac{2C_2}{H}\left(\mathrm{ch}(\mathrm{H}) - \mathrm{ch}(\mathrm{H}Z)\right) \right] + \tilde{r}(1 - Z^2) \tag{21}$$

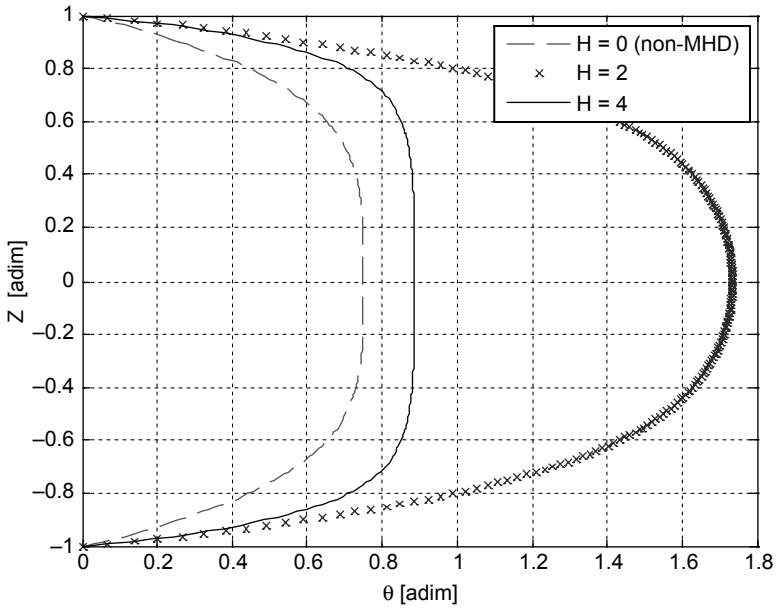

Figure 5 Analytical temperature distribution for the Hartman problem (with K*u=100).

where constants C_1 and C_2 are given by $C_1 = \left(\frac{\mathrm{H}}{\mathrm{H\,ch(H)} - \mathrm{sh(H)}} \right)^2$ and $C_2 = H(K–1)\mathrm{ch(H)}–K\mathrm{sh(H)}$. The temperature profile according to Eq. (21) is represented by Fig. 5 for various values of the Harman number H.

According to [11], it is also of interest to note that if the heat flux q_w at the wall is independent of x and the problem is assumed to be one-dimensional, then T must be a linear function of x:

$$T(x) = kx + g(z) \tag{22}$$

with the boundary condition expressed as $\frac{dg}{dz}(\pm a) = q_w$.

Substituting Eq. (22) in Eq. (20) yields $g(z)$ and θ, hence $k = \frac{q_w + \int_{-a}^{+a} (\eta \left(\frac{\partial u_x}{\partial z} \right)^2 + \frac{j_y^2}{\sigma}) dz}{\rho \bar{u} c_v a}$.

It can be inferred that if $q_w = -\int_{-a}^{+a} (\eta \left(\frac{\partial u_x}{\partial z} \right)^2 + \frac{j_y^2}{\sigma}) dz$, then $k = 0$ and the previous problem solution is recovered since in this case, all the heat generated by viscous and Joule dissipation is transferred out of the channel. When q_w is not constant or with a non-linear variation of T along the channel wall, the problem become two-dimensional and rise many more difficulties [9].

When the thermal conductivity is a function of T, the previous equation of energy (8) has to be modified in (23):

$$\frac{\rho}{\lambda}\frac{De}{Dt} = \Delta T + \frac{d\lambda_{(T)}}{dT}\left(\nabla T\right)^2 + \frac{\eta}{\lambda}\left\|\nabla \mathbf{v} + \nabla \mathbf{v}^T\right\|^2 + \frac{\mathbf{j}\cdot\mathbf{E}}{\lambda} + \frac{r}{\lambda} \tag{23}$$

The thermal conductivity of the fluid is assuming here to be a linear function of T:

$$\lambda(T) = A_0 + A_1 T = A_0 + A_1(T_w + \theta\frac{\overline{u}^2}{c_v}) = \tilde{A}_0 + \tilde{A}_1\theta \tag{24}$$

Then, with $e = C_v T$ and the previous boundary condition for T, (23) can be solved with the Hartmann velocity profiles founded upper:

$$\theta_1 = -\frac{1}{\varepsilon_1} + \frac{1}{\varepsilon_1}\sqrt{1 + 2\varepsilon_1\left[C_1 \mathrm{P}_{\mathrm{r}0}\left(\frac{C_2^2(1-Z^2)}{2} + \frac{\mathrm{ch}(2\mathrm{H}) - \mathrm{ch}(2\mathbf{H}Z)}{4} + \frac{2C_2\,\mathrm{ch}(\mathrm{H}) - \mathrm{ch}(\mathrm{H}Z)}{\mathrm{H}}\right) + \frac{\tilde{r}_0(1-Z^2)}{2}\right]} \tag{25}$$

where $\mathrm{P}_{\mathrm{r}0} = \dfrac{\eta c_v}{\tilde{A}_0}$ is the Prandtl number at order 0 in $\varepsilon_1 = \dfrac{\tilde{A}_1}{\tilde{A}_0}$, and $\tilde{r}_0 = r\dfrac{c_v a^2}{\tilde{A}_0 \overline{u}^2}$, which allows to recover the previous solution, with a constant λ, at order 0 in ε_1, and then to obtain the gap between the two solutions at order 1 in ε_1, hence $E_{\max} = E(Z=0) \approx -\dfrac{\theta_0^2(Z=0)}{2}\varepsilon_1$.

3.2. NUMERICAL SIMULATION FOR THE HARTMANN PROBLEM: RESULTS AND VALIDATION

The CFD problem can be solved in two dimensions, which has been performed within the COMSOL-Multiphysic environment: a two-dimensional duct with a length of 15 m to minimize end effects and a wide of 10 cm to avoid apparition of secondary flows is considered for that purpose. This duct is meshed with 5124 triangular finite elements. Boundary conditions are a uniform and constant pressure at inlet and outlet, a constant and uniform magnetic field B_o = 1 mT normal to the plane of the flow, a tension of Ω = 10 mV between the two electrodes, a null wall temperature, and a conductor fluid.

The fluid has the following physical-chemical parameters: ρ = 998 kg/m^3, η = 10–3 Pa.s λ = 5 W/m/K, C_v = 100 J/kg, σ = 10 S/m. Accordingly, the Reynolds number for the fluid flow is R_e = 42, which allows to solve the Navier-Stokes equations without taking turbulent effects into account. The magnetic Reynolds number is equal to $\mathrm{R}_m = 8 \cdot 10^{-10}$, which indicates that the feedback of the fluid motion on the magnetic field is limited. The Hartmann number is $H = 5 \cdot 10^{-3}$ which means the MHD aspect of the flow is not strong, and the load factor $K = 1{,}2 \cdot 10^5$ indicates that the duct is working as a pump. One can notice that with a purely hydrodynamic problem, there will be no flow through the duct.

The CFD simulation is compared to a classical analytical solutions described in [1], on Figs. 6 and 7. The results show an excellent agreement between the CFD profiles and the analytical solutions, both in terms of velocity profiles and temperature distribution, which yields the validation of the numerical procedure for this elementary test case.

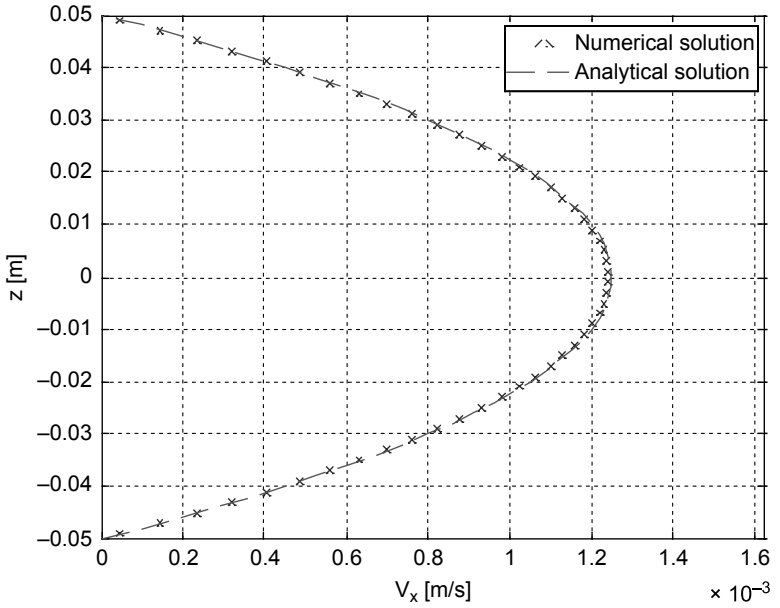

Figure 6 Analytical and numerical velocity profiles for the Hartmann problem.

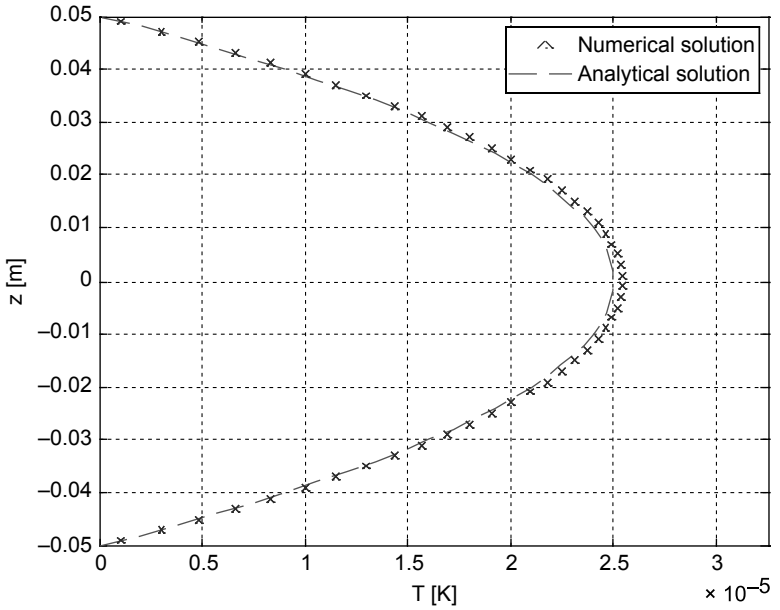

Figure 7 Analytical and numerical temperature distribution for the Hartmann problem.

4. COUETTE PROBLEM

The second elementary test case considered in the present investigation is the so-called "Couette problem", represented in Fig. 8 below. In such problem; the lower wall at $z = 0$ remains stationary, while the upper wall at $z = L$ is moving with a constant velocity $u(L) = u_w$.

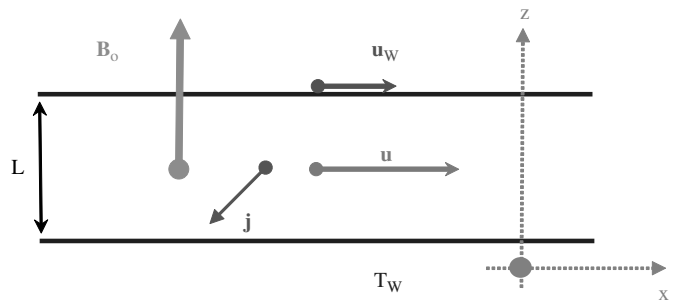

Figure 8 Definition of the MHD "Couette problem".

The "Couette problem" problem is therefore more general than the "Hartman problem" considered in the previous section; the latter can be viewed as a particular car of the former with $u_w = 0$.

Since this problem is quite similar to the previous one, the same hypothesis hold, namely $\mathbf{v} = (u_x, 0, 0)$, $\mathbf{j} = (0, j_y, 0)$, $\mathbf{B} = (b_x, 0, B_o)$, $\mathbf{E} = (0, E_o, 0)$, where E_o and B_o are constants.

4.1. ANALYTICAL SOLUTION FOR THE COUETTE PROBLEM

As in the previous section, the heat-transfer and the fluid motion equations are uncoupled, and it is possible to solve equations separately. Moreover the equations are linear and, following e.g. [3], the solution for u is found to be:

$$U = \frac{u_x}{u_w} = K + \frac{\left(1-K\right)\mathrm{sh}\left(\mathrm{ZH}\right) - K\,\mathrm{sh}\left[\mathrm{H}\left(1-Z\right)\right]}{\mathrm{sh}\left(\mathrm{H}\right)} \tag{26}$$

$$\frac{\bar{u}}{u_w} = K + \left(1-2K\right)\frac{1}{\mathrm{H}}\,\mathrm{th}\left(\frac{\mathrm{H}}{2}\right) \tag{27}$$

with boundary conditions $u(0) = 0$, and $u(L) = u_w$.The non-dimensional numbers appearing in Eqs. (26) and (27) are defined as follows: $Z = \frac{z}{L}$, $\mathrm{H} = aB_o\sqrt{\frac{\sigma}{\eta}}$ and $K = \frac{E_o}{u_w B_o}$.

Figure 9 plots some typical velocity profile within the duct in the Couette problem, for various H; it is stressed that the case H = 0 corresponds to the situation where magnetic forcing is absent.

In the same manner as is derived in the previous section, the following relationship are retrieved:

$$\tilde{j}_y = \frac{j_y}{\sigma\bar{u}B_o} = K - \frac{u_x}{\bar{u}} = K - U \tag{28}$$

$$E_o = \frac{\Omega}{2b} \tag{29}$$

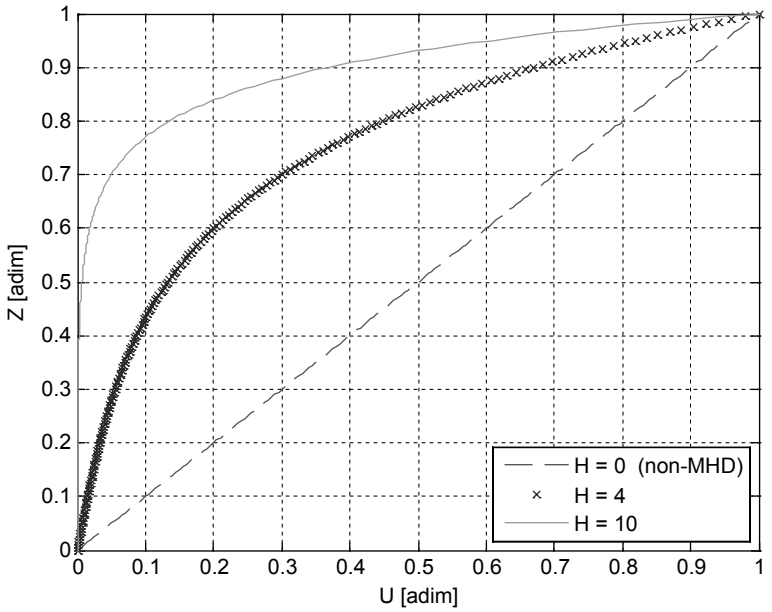

Figure 9 Couette flow velocity analytical profiles (K=0).

$$\tilde{b}_x = \frac{b_x}{B_o \mathrm{R_m}} = \frac{\mathrm{ch(H)} - \mathrm{ch}(Z\mathrm{H})}{\mathrm{H\ sh(H)}} \tag{30}$$

with boundary condition $b_x(L) = 0$. Letting $e = C_v T$, the boundary condition for T is assumed to be: $T(0) = T_w$ and $T(L) = T_w$. As a consequence, using the reduced temperature $\theta = \frac{C_v}{u_w^2}(T - T_w)$, the solution of (8) is:

$$\theta_2 = \frac{\mathrm{P_r}}{4\mathrm{sh}^3(\mathrm{H})}\left[\frac{K^2-4K+2}{2}\mathrm{sh}(\mathrm{H}) + \frac{1-2K}{2}\mathrm{sh}\left(\mathrm{H}(2Z-1)\right) + \left(K^2-K\right)\left[\mathrm{sh}(2Z\mathrm{H}) - \mathrm{sh}(2\mathrm{H})\right]\right.$$
$$\left. - \frac{(K-1)^2}{2}\mathrm{sh}\left(\mathrm{H}(2Z+1)\right) + K(1-K)\mathrm{sh}\left(2\mathrm{H}(Z-1)\right) + \frac{\mathrm{K}^2}{2}\left[\mathrm{sh}\left(\mathrm{H}(2Z-3)\right) + \mathrm{sh}(3\mathrm{H})\right]\right]$$
$$+\left[\mathrm{P_r}\frac{1-2K}{2} + \frac{\tilde{r}(1-Z)}{2}\right]Z$$

where $\mathrm{P_r} = \frac{\eta C_v}{\lambda}$ and $\tilde{r} = r\frac{C_v a^2}{\lambda u_w^2}$.

The temperature profile according to Eq. (31) is represented by Fig. 10 for various values of the Harman number H.

It is also interesting to know that an analytical solution for the temperature distribution of a Couette flow has also been found when λ is a linear function of T, but the solution has too many terms to be reproduced here.

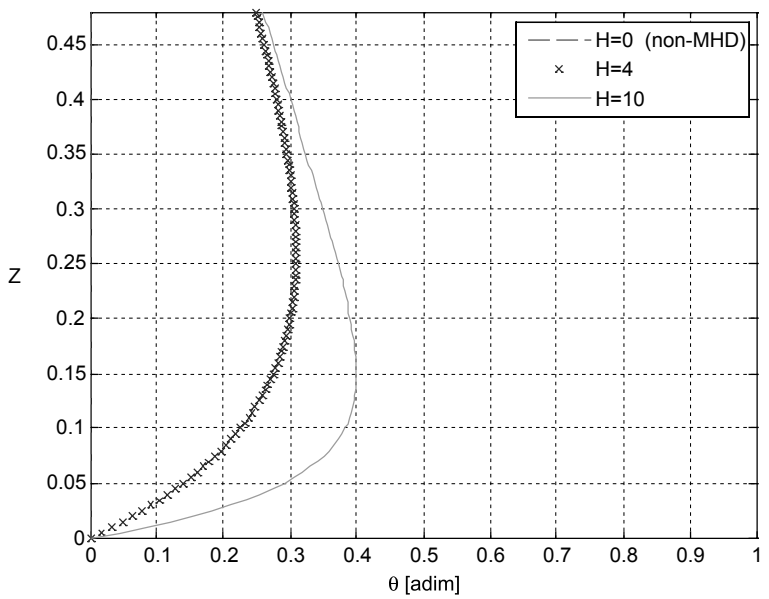

Figure 10 Couette flow temperature analytical distribution (K*u=100).

4.2. NUMERICAL SIMULATION FOR THE COUETTE PROBLEM: RESULTS AND VALIDATION

In the same manner as for the Hartman problem, a CFD procedure can be used to solve the problem in two dimensions; a two-dimensional duct with a length of 17 m to minimize end effects and a wide of 10 cm to avoid apparition of secondary flows, is considered. This duct is meshed with 9722 triangular finite elements. The boundary conditions are a uniform and constant pressure inlet and outlet, a velocity of u_w = 0,01 mm/s for the upper wall, a constant and uniform magnetic field B_o = 0.1 mT, a tension of Ω = 0.2 mV between the two electrodes, a wall temperature null, and a conductor fluid. The fluid has the following physical-chemical parameters: ρ = 998 kg/m^3, $\eta = 10^{-3}$ Pa.s, λ = 0.6 W/m/K , C_v = 4187 J/kg, σ = 10 S/m.

Accordingly, the Reynolds number of the fluid flow is R_e = 1, which allows to solve the Navier-Stokes equations without a turbulent model. The magnetic Reynolds number is equal to $R_m = 10^{-11}$, so that the feedback of the fluid motion on the magnetic field is rather weak. The Hartmann number is $H = 1 \cdot 10^{-3}$, which indicates that the MHD aspect of the flow is not strong; and the load factor $K = 2 \cdot 10^6$ indicates that the duct is working as a pump. One can notice that with a purely hydrodynamic problem, there will be no flow through the duct.

The results of the CFD simulation is compared to classical analytical solutions described in [1]. Figure 11 shows that the agreement for the velocity profile is good on all the wide of the duct. It can also be noticed that the MHD aspect is clearly visible through the non-linear shape of the profile. As far as the temperature distribution is concerned, it can be concluded that the end effects are stronger than those of velocity; accordingly, the temperature is slightly over-estimated by the numerical simulation, as we can be inferred from Fig. 11. Additional numerical tests are carried out in the framework of the present study, but not reported in the paper for the shake of brevity; they evidences that it is possible to improve the temperature estimation using a larger computational domain, as could be expected *a priori*.

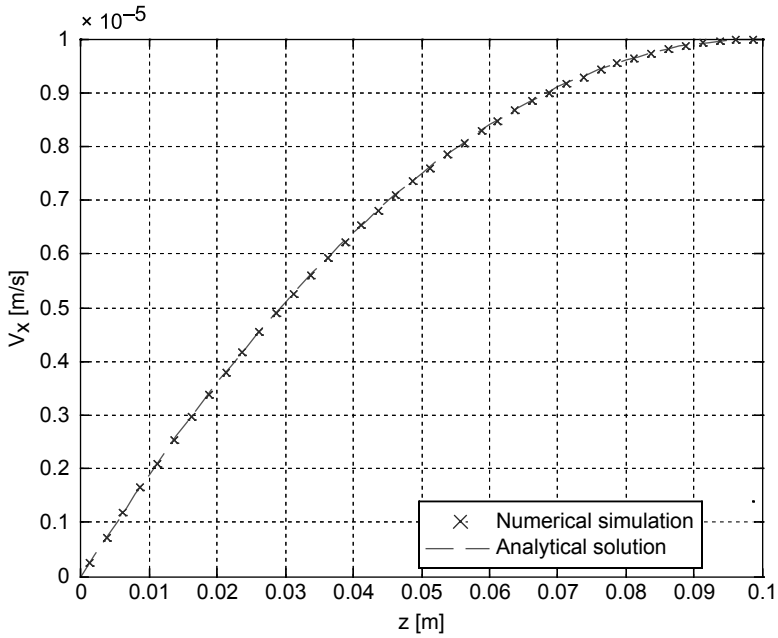

Figure 11 Analytic and CFD velocity profiles for the Couette problem.

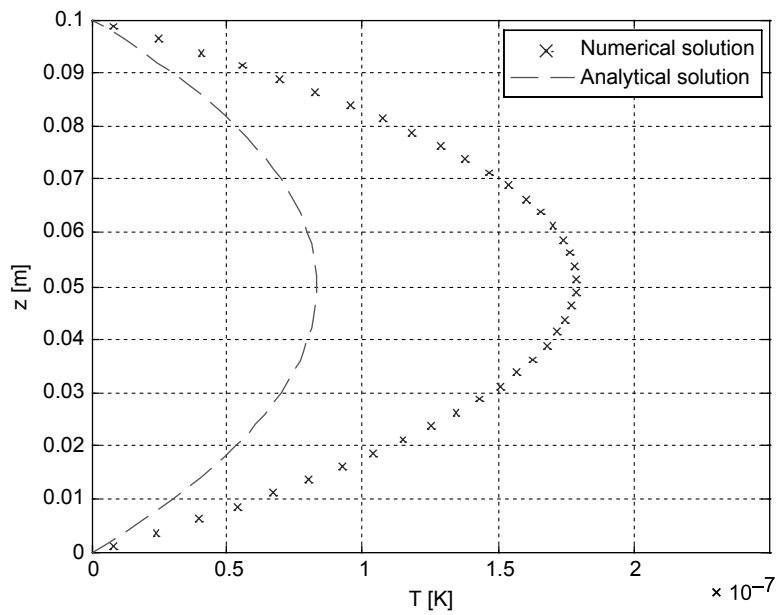

Figure 12 Analytic and CFD temperature distribution for the Couette problem.

5. RAYLEIGH PROBLEM

The third elementary test case considered in the present investigation is the so-called "Rayleigh problem", represented in Fig. 13 bellow. Such configuration corresponds to a transient problem in which a magnetic field, assumed uniform in space and constant in time,

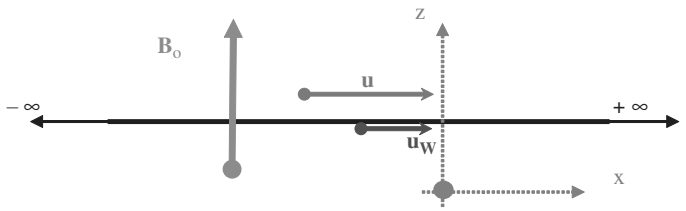

Figure 13 Rayleigh problem configuration.

is applied normal to the surface of an impulsively moved half plane. This problem is of particular interest because an analytical solution can be obtained in closed form, so that the nature of Magneto-Hydro-Dynamic boundary-layer can be investigated. Moreover, this problem is a complementary test case which allows considering transient flow configurations.

5.1. ANALYTICAL SOLUTION FOR THE RAYLEIGH PROBLEM

Because of the transient nature of the problem, it is convenient to solve the problem with the so-called "induction equation", which reads:

$$\frac{D\boldsymbol{B}}{Dt} = \left(\boldsymbol{B}\cdot\boldsymbol{\nabla}\right)\boldsymbol{v} + D_{\text{mag}}\cdot\Delta\boldsymbol{B} \tag{33}$$

and which is obtained directly from the Maxwell and Ohm equations. Governing equations of the problem are (7) and (33), which are reformulated in the case of Fig. 13:

$$\rho\frac{\partial u}{\partial t} = \frac{B_o}{\mu}\frac{\partial b_x}{\partial y} + \eta\cdot\frac{\partial^2 u}{\partial y^2} \tag{34}$$

$$\frac{\partial b_x}{\partial t} = B_o\frac{\partial u}{\partial y} + D_{\text{mag}}\frac{\partial^2 b_x}{\partial y^2} \tag{35}$$

Following [3], initial values and boundaries conditions are as follows: $u(y,0) = 0$, $b_x(y,0) = 0$, $u(0,t) = u_o$, $b_x(0,t) = 0$ with u and b_x being bounded when $y \to \infty$.

As in the previous section, the heat-transfer and fluid motion equations are uncoupled and it is possible to solve equations separately. However, equations (34) and (35) show that the velocity and the induced magnetic field are solutions of a partial differential system of two coupled equations. A general expression of the shear stress on the wall can be obtained, see for instance [3]:

$$\tau_w(t) = \frac{\eta u_0}{\sqrt{\nu}}\left[\frac{e^{-\gamma\cdot t}}{\sqrt{\pi t}} + \sqrt{\gamma}\,\text{erf}\left(\sqrt{\gamma t}\right)\right] \underset{t\to\infty}{\longrightarrow} \frac{\sqrt{\text{P}_\text{m}}}{1+\sqrt{\text{P}_\text{m}}} \tag{36}$$

where $\gamma = \dfrac{\sigma B_o^2}{\rho\left(1+\sqrt{\text{P}_\text{m}}\right)^2}$.

It is also possible to derive a general solution for the steady motion because in this case, (34) and (35) can be written as:

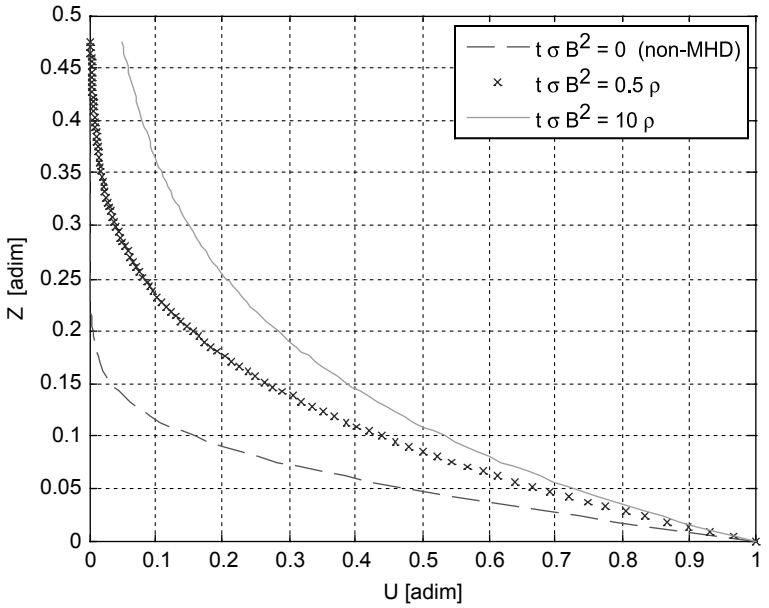

Figure 14 Velocity profiles in the Rayleigh problem.

$$0 = \frac{B_o}{\mu}\frac{\partial b_x}{\partial z} + \eta\frac{\partial^2 u}{\partial z^2} \tag{37}$$

$$0 = B_o\frac{\partial u}{\partial z} + D_{\text{mag}}\frac{\partial^2 b_x}{\partial z^2} \tag{38}$$

The latter which can be solved:

$$U = \frac{u}{u_0} = e^{-\frac{y}{L}} \tag{39}$$

$$b_x = \sqrt{\sigma\eta}u_0\mu\left(U-1\right) \tag{40}$$

where $\mathrm{L} = \frac{1}{B_o}\sqrt{\frac{\eta}{\sigma}}$ is a characteristic length of the problem.

However, no general solution can be found for the Rayleigh problem, and hypotheses have to be made to go further. Various approximations can be made, see for instance references [6] and [7]; in the present case, it is assumed that $\mathrm{R_m} << \mathrm{R_e}$. Using this hypothesis, and following [3], it is possible to derive and analytical expression for the velocity field in the frequency domain with the aid of the Laplace transform; turning back into the temporal domain, the solution reads:

$$U = \frac{u_x}{u_0} = \frac{1}{2}\left[e^{-\frac{y}{L}}\cdot\operatorname{erfc}\left(\frac{y}{2\sqrt{\nu t}} - \sqrt{\frac{\sigma B_{ot}^2 t}{\rho}}\right) + e^{\frac{y}{L}}\cdot\operatorname{erfc}\left(\frac{y}{2\sqrt{\nu t}} + \sqrt{\frac{\sigma B_o^2 t}{\rho}}\right)\right] \tag{41}$$

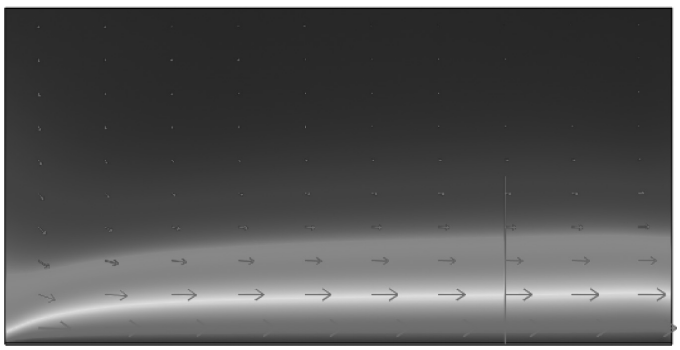

Figure 15 Visualisation of the flow for the Rayleigh problem.

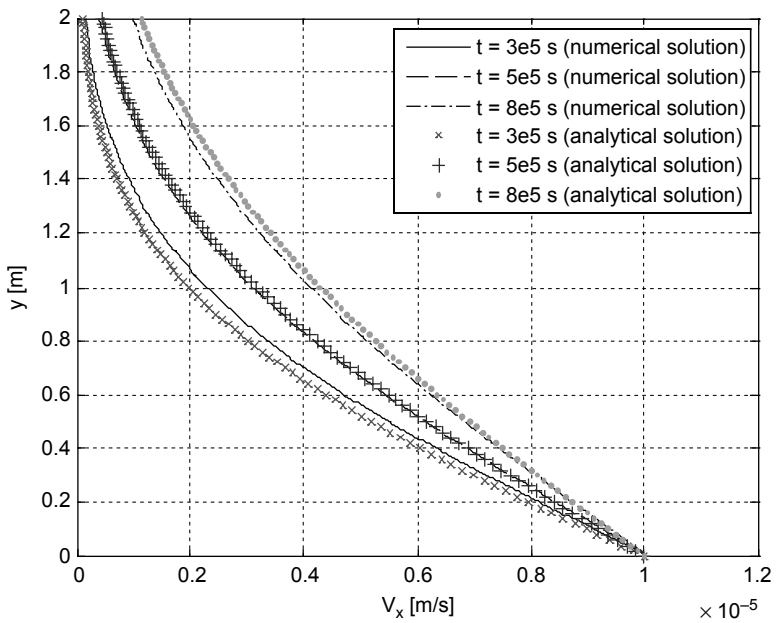

Figure 16 Analytical and CFD velocity profiles for the "Rayleigh problem" at different times.

Figure 14 plots some typical velocity profile within the duct in the Rayleigh problem, for various values of $t\sigma B_o^2$; it is stressed that the case $t\sigma B_o^2 = 0$ corresponds to the situation where magnetic forcing is absent.

Taking into account magnetic effects has direct influence on the numerical simulation, since it is observed that the computational effort increases together with the magnetic field intensity. The asymptotic expression of Eq. (41) allows recovering the classical solution of this problem:

$$H << 1 : U = \frac{u}{u_0} = \operatorname{erfc}\left(\frac{y}{2\sqrt{\nu t}}\right) \tag{42}$$

The study of the temperature distribution is a boundary layer problem, which is quite difficult to solve analytically; it has however been already discussed by several authors, see for instance reference [ ]. As it is far beyond the purpose of the present work, it will therefore not be considered here in details.

5.2. NUMERICAL SIMULATION FOR THE RAYLEIGH PROBLEM: RESULTS AND VALIDATION

CFD calculations are performed in the same manner as for the Hartman and Couette problems, using the COMSOL-Multiphysic software. In the present simulations, the velocity of the wall is set to u_w = 0.01 mm/s, while all other parameters are the same as those used for the Couette problem.

As in the former cases, the results of the CFD simulation are compared to classical analytical solutions, as described in [1]. Figure 15 evidences the link between the fluid flow and a boundary layer, while a comparison between the analytical solution and the numerical solution is proposed on Fig. 16. The latter shows a good agreement between the analytical and numerical solutions, even after for long times, which allows validating the numerical tool and procedures for further engineering applications.

6. CONCLUSION

In the present paper, three different test cases for Magneto-Hydro-Dynamic problems have been investigated, both from the analytical and numerical standpoints. The so-called "Hartmann problem", "Couette problem" and "Rayleigh problem" serve as validation test case in MHD configuration.

Analytical solution for the fluid velocity profile as well as for the temperature profile have firstly been derived for each problem; numerical simulations have secondly performed using an engineering numerical tool for multi-physic applications, namely the COMSOL-Multiphysic code; comparisons between analytical and numerical solutions have thirdly been performed.

The present work serves as starting point for further studies which will be performed with the COMSOL-Multiphysic code for industrial-oriented problems. It can also be viewed as a reference work for validation of coupled numerical procedures for academic studies.

NOMENCLATURE

t = time
$\mathbf{V}$ = velocity vector
u = horizontal velocity
$\underline{?}$ = average horizontal velocity
$\mathbf{E}$ = electric field vector
$\mathbf{B}$ = magnetic field vector
$\mathbf{j}$ = current density
J = net current through the circuit per unit area
Z = non-dimensional height
U = non-dimensional velocity
T = absolute temperature
p = pressure in the fluid
ρ = density of the fluid
σ = electrical conductivity of the fluid
μ = absolute magnetic permeability

ε = absolute magnetic permittivity
λ = thermal conductivity of the fluid
C_v = specific heat at constant volume
η = Dynamic viscosity of the fluid (Pa s in SI)
ν = kinematical viscosity of the fluid
$\mathbf{D}_r$ = remanent displacement
$\mathbf{B}_r$ = remanent magnetic flux density
ρ_e = electric charge density
V = electric potential
Ω = electric tension (electric potential gap between the two electrodes)
e = energy per unit mass of the fluid and
r = volumic source of heat
R_e = reynolds number
R_m = magnetic Reynolds number
D_{mag} = magnetic diffusivity
H = Hartmann number
K = load factor
P_r = Prandtl number
θ = reduced temperature

REFERENCES

[1] R. Berton. *Magnétohydrodynamique*. Masson, 1991.

[2] T. G. W. Cowling. *Magnetohydrodynamics*. Interscience Publishers, 1957.

[3] G. W. Sutton, A. Sherman. *Engineering Magnetohydrodynamics*. Dover, 2006.

[4] D. Convert. *Propulsion magnétohydrodynamique en eau de mer.* Thèse de Doctorat, Université de Grenoble, 1995.

[5] P. Boissonneau, J.P. Thibault. Experimental analysis of coupling between electrolysis and hydrodynamics in the context of MHD in seawater. *Journal of Physics. D, Applied Physics,* 32, 2387–2398, 1999.

[6] G. S. S. Ludford. Rayleigh's Problem in Hydromagnetics : The Impulsive Motion of a Pole Piece. *Archive in Rationnal Mechanical Analysis,* 3 (14), 1959.

[7] V. J. Rossow. *On Flow of electrically conducting fluids over a flat plate in the presence of a transverse magnetic field*. NASA Report #1358, 1958.

[8] D. L. Mitchell, D.U. Gubser. Magnetohydrodynamic ship Propulsion with Superconducting Magnets. *Journal of Superconductor,* 1, 349–364, 1988.

[9] S. D. Nigam, S.N. Singh. Heat transfer by laminar flow between parallel plates under the action of transverse magnetic field. *Quartly Journal of Mechanical & Applied Mathematics,* 13, 85–97, 1960.

[10] M. Zakaria. Thermal boundary layer equation for a magnetohydrodynamic flow of a perfectly conducting fluid. *Applied Mathematics and Computation,* 148, 67–79, 2004.

[11] J. Lohrashbi. Magnetohydrodynamic heat transfer in two-phase flow between parallel plates. *Applied Scientific Research,* 45, 53–66, 19 88.